Advances in turbulence measurements using new Correlation ECE and nT-phase diagnostics at ASDEX Upgrade

Simon J. Freethy[1,2], *Tobias* Görler[1], *Alex J.* Creely[2], *Garrard D.* Conway[1], *Severin S.* Denk[1,3], *Tim* Happel[1], *Pascale* Henniquin[4], *Christian* Koenen[5], *Anne E.* White[2], and *The ASDEX Upgrade* team[1]

[1]Max Plank Institute for Plasma Physics, 85748 Garching, Germany
[2]Plasma Science and Fusion Center, Massachusetts Institute of Technology, Cambridge, MA 02139, USA
[3]Physik-Department E28, Technische Universität München, 85748 Garching, Germany
[4]Laboratoire de Physique des Plasmas, Ecole Polytechnique, 91128, Palaiseau cedex, France
[5]Lehrstuhl für Hochfrequenztechnik, Technische Universität München, Arcisstr. 21, 80333 München

Abstract. Guided by predictions from nonlinear gyrokinetic simulations, two new turbulence diagnostics were designed and installed at ASDEX Upgrade (AUG) to probe the fundamentals of ion-scale turbulent electron heat transport. The first, a 30-channel correlation ECE (CECE) radiometer (105-128 GHz, 2nd harmonic X-mode), introduces a novel channel comb arrangement. This allows measurements of high radial resolution profiles ($0.5 < r/a < 0.8$) of low-k ($k_\theta \rho_s < 0.3$) temperature fluctuation amplitudes, frequency spectra and radial correlation length profiles in unprecedented detail. The second diagnostic is formed by the addition of two W-band and one V-band X-mode reflectometers on the same line of sight as the CECE to enable measurements of the phase angle between turbulent density and temperature fluctuations α_{nT}. Historically, the radial alignment between reflectometer and radiometer has been a challenge due to the requirement that alignment is achieved within a radial correlation length ($< 5 - 10$ mm). This challenge is significantly alleviated by using the CECE channel comb arrangement and the maximal coherence between reflectometer and radiometer can be unambiguously captured. Measurements of these quantities have been made in an AUG L-mode plasma, at the same radial location and have provided simultaneous quantitative constraints on realistic gyrokinetic simulations [Physics of Plasmas **25**, 055903 (2018)] using the gyrokinetic code GENE and this proceedings presents diagnostic detail for this study.

1 Introduction

Understanding the turbulent driven heat flux in a tokamak remains one of the key goals of fusion research. Anomalous transport up to two orders of magnitude above what one would expect from neoclassical theory is observed and this is now understood to be caused by turbulent fluctuations in the plasma density, temperature and potential, originating from drift-wave like instabilities which grow and non-linearly saturate [1, 2]. The heat flux driven by these fluctuations depends not only on the amplitudes of the fluctuating quantities, but on their relative coherencies and phase angles [3]. Experimental measurements of these cross-field quantities are rare due to the difficulty in attaining them, but offer extremely valuable information with which to constrain high fidelity models of turbulence. The phase angle between temperature and density fluctuations α_{nT} has been measured in the core plasma by the combination of a reflectometer and radiometer [3, 4] and has subsequently been shown to vary as a function of the normalised electron temperature gradient [5]. Recent work with gyrokinetic models has also shown that the average α_{nT} is a good experimental measure of the balance of ion temperature gradient driven (ITG) and trapped electron driven (TEM) structure [6]. This is invaluable information as a quantitative constraint on turbulence models where both modes are present, as the electron and ion heat flux (Q_e and Q_i) must be matched for the same combination of inputs as α_{nT} is matched. That is to say one cannot independently vary the mix of ion and electron modes to match Q_e and Q_i. A validation study of the GENE gyrokinetic code [7] has shown that an ion scale model for a medium density, electron heated AUG L-mode plasma is able to simultaneously match Q_e, Q_i, α_{nT} and the radial correlation length $L_r(T_{e\perp})$, while moderately over predicting the temperature fluctuation amplitude $\delta T_{e\perp}/T_e$.

Here we describe in more detail the novel correlation ECE (CECE) and α_{nT} diagnostics used to make the measurements described in the above study. A significant problem in the operation of a combination reflectometer radiometer α_{nT} diagnostic is the stringent radial alignment constraint. The frequency of the reflectometer should be chosen with sufficient accuracy such that the cut-off position aligns well within a turbulent radial correlation length of an ECE radiometer channel, i.e. < 5 mm. Within the uncertainties of the experiment, this is impossible to achieve a priory for a single radiometer channel. In order to directly address this issue, of the 28 channels of the AUG CECE diagnostic, 24 channels are arranged in a frequency comb designed to give continuous spatial coverage over a small radial region. This is sufficient to achieve radial alignment using only a single plasma discharge, thus significantly improving the reliability, productivity and usefulness of the diagnostic.

Measurements of $L_r(T_{e\perp})$ have been previously performed [8, 9], but measurements of this quantity are rare. These measurements are also often composed of an ensemble of measurements made over a large radial range, where $L_r(T_{e\perp})$ would be expected to vary. The AUG CECE channel comb allows high resolution $L_r(T_{e\perp})$ profiles to be measured for the first time. This data can then be used to show for the first time that $L_r(T_{e\perp}) \propto \rho_s$, as has been shown for density fluctiations [10]. The CECE diagnostic is described in Section 2 along with $L_r(T_{e\perp})$ profiles and the α_{nT} diagnostic and analysis technique is described in Section 3.

2 Correlation ECE diagnostic

In order to investigate the ion-scale electron heat transport at ASDEX Upgrade, a Correlation ECE receiver was designed and built which employs both a high channel number and a novel channel comb arrangement. Three interchangable radio frequency (RF) sections employ tunable oscilators in the range 105.5-109.1 GHz, 110.2-113.8 GHz and 113.5-117 GHz, which in turn feed a filter bank of 24 fixed channels covering the range 4-8 GHz in steps of either 100 or 200 MHz. This results in a radial spacing on the order of the ECE linewidth ensuring maximal spatial resolution of between 2-4mm. Four additional tunable YiG filters increase the frequancy range up to 14GHz. This configuration was guided by ECE modelling using a radiation transport model [11] and existing non-linear gyrokinetic (GK) simulations for predictions of the radial correlation length of the perpendicular electron temperature fluctuations $L_r(T_{e\perp})$.

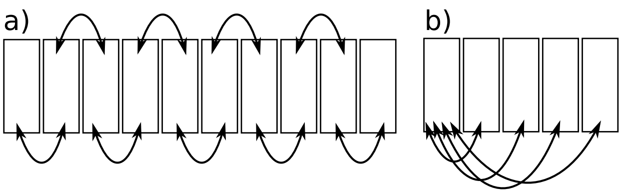

Figure 1. Examples of correlation patterns for high radial resolution $\delta T_e/T_e$ profiles (a) and correlation length measurements (b). Adapted from [6].

The novel channel comb allows the measurement of high resolution $\delta T_{e\perp}/T_e$ and $L_r(T_{e\perp})$ profiles. $\delta T_{e\perp}/T_e$ is calculated from a nearest neighbour cross-correlation as shown in Figure 1 (a). The correlation length is calculated from cross-correlations of increasing distance as shown in Figure 1 (b). In this case, the reference channel can be changed and the process repeated, allowing a correlation length profile to be built up. Figure 2 shows $\delta T_{e\perp}/T_e$ and $L_r(T_{e\perp})$ profiles for a medium density L-mode plasma with $T_e > T_i$. It has previously been reported for density fluctuations that $L_r(n_e) \simeq 5 - 10\rho_s$ [10]. We can use this data

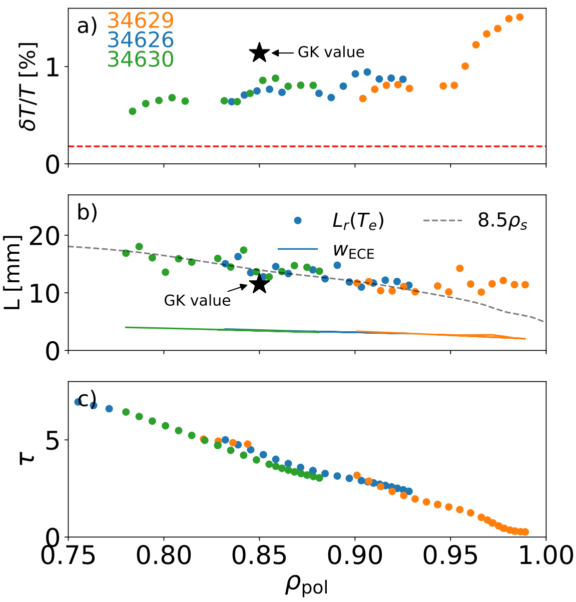

Figure 2. High radial resolution $\delta T_{e,\perp}/T_e$ profile (a) and correlation length profile, $L_r(T_{e\perp})$, (b) as measured by the AUG CECE diagnostic. $L_r(T_{e\perp})$ is shown to agree well with $8.5\rho_s$ in this case, with a jump at $\rho_{\rm pol} = 0.95$. The ECE linewidth $w_{\rm ECE}$ and gyrokinetic values are also shown for comparison. Panel (c) shows the optical depth for these measurements.

to confirm for the first time a similar trend for the electron temperature fluctuations. In our case $L_r(T_{e\perp}) = 8.5\rho_s$, as shown in Figure 2 (b).

Non linear gyrokinetic results for these quantities at $\rho_{\rm pol} = 0.86$ produced using the GENE gyrokinetic code [7] and described in a previous publication [6] are also shown in the figure, denoted by the black stars. As you can see, reasonable agreement between GENE and the experiment is found, although the code slightly over predicts $\delta T_{e,\perp}/T_e$.

3 nT cross-phase diagnostic

The cross-phase angles between the fluctuating fields are important quantities for the validation of gyrokinetic models, since they determine the magnitude of the heat flux along with the fluctuation amplitudes. The most experimentally accessible quantity for core fluctuations is the phase angle between temperature and density fluctuations. This quantity has been measured using a combination of a reflectometer for the density fluctuations and a radiometer for the temperature fluctuations, which share the same line of sight to the plasma [3]. This quantity has also been shown to vary when experimentally varying the T_e normalised gradient scale length $1/L_{Te}$, which is a drive for the trapped electron mode (TEM) [5]. This work indicates that α_{nT} is an experimental measure of the balance of TEM and ITG structure present in the turbulence.

The α_{nT} diagnostic developed at AUG makes a considerable improvement to the reliability and interpretation

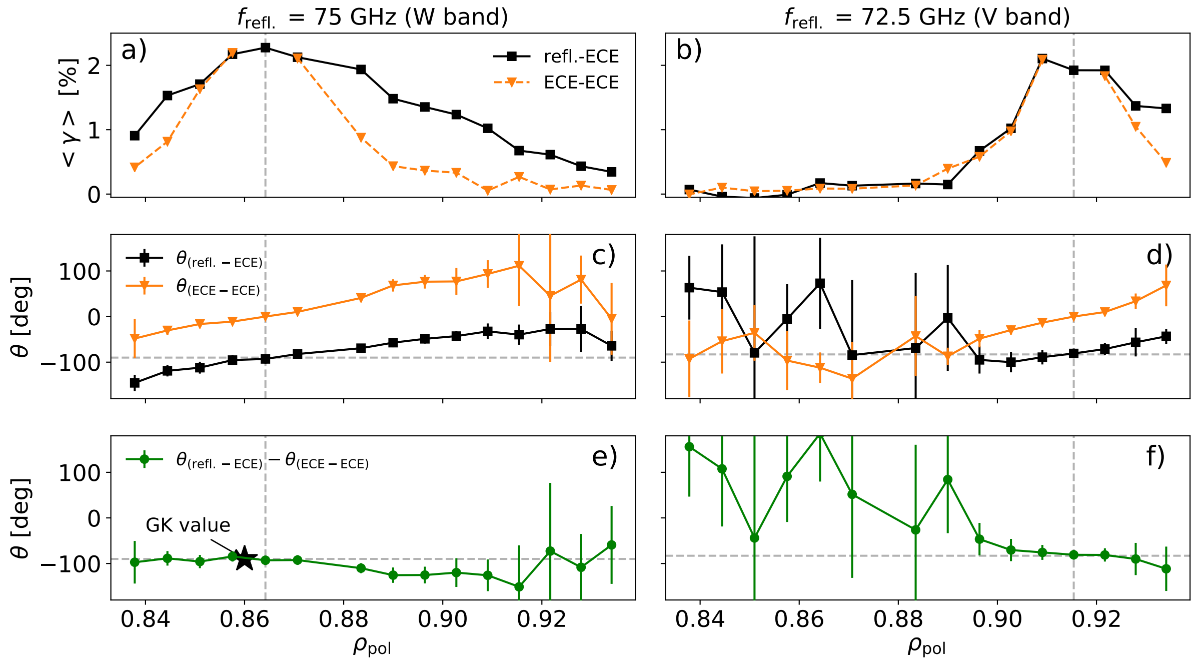

Figure 3. (a) and (b): Coherence between ECE channels (orange triangles) and ECE and reflectometer amplitude (black squares) averaged between 0-100 kHz for reflectometer probing frequency of 75 GHz and 72.5 GHz. The ECE coherence is scaled by 0.4. (c) and (d): The cross phases averaged between 10-40 kHz between the ECE channels (orange triangles), ECE and reflectometer amplitude (black squares). (e) and (f) The difference between ECE-ECE average cross-phase and refl.-ECE cross phase. There is clearly a linear trend of the cross phase with radius, which is reproduced in both the CECE measurement and the nT-phase measurement.

of the measurement, by making use of the CECE channel comb. An X-mode reflectometer illuminates the plasma at a fixed frequency, and the resulting amplitude fluctuations in the return wave are correlated with each of the CECE channels in turn. It is then possible to build up a profile of the coherence between reflectometer and radiometer (refl.-ECE) as shown in Figure 3 (a) and (b). These panels show the coherence averaged between 0-100 kHz for refl.-ECE (black squares) and between radiometer channels (ECE-ECE, orange triangles) with respect to a reference channel chosen to line up with the peak refl.-ECE coherence. The width of the latter is dominated by the $L_r(T_{e\perp})$ as shown in section 2. One can see that the refl.-ECE coherence function is asymmetric, being broader towards higher radii compared to the ECE-ECE coherence function. This is due to the fact that the reflectometer scattering carries information about density fluctuations away from the cut-off location and is thus correlated with fluctuations more than a radial correlation length away from the cut-off.

Figure 3 (c) and (d) show the cross-phase averaged from 10-40 kHz for refl.-ECE correlations (black squares), ECE-ECE correlations (orange triangles). One can see that there is a slope in the average cross-phase present both in ECE-ECE and refl.-ECE correlations and this is due to a finite radial time delay of the turbulent structures. This is considered to originate from the finite turbulent eddy tilt angle, as there is no poloidal projection to this line of sight. Both refl.-ECE and ECE-ECE correlations show approximately the same phase behaviour with radius. Subtracting $\theta_{\text{ECE}-\text{ECE}}$ from $\theta_{\text{refl.}-\text{ECE}}$, as shown in panels (e) and (f), shows a flat region around the peak coherence which is due to the cross-phase between temperature and density fluctuations, α_{nT}.

The advantage of the channel comb is then clear in the presence of such a behaviour in the cross-phase, as the ECE-ECE correlations are required to correct the phase trend in the refl.-ECE correlations for a robust measurement. Further, the measurement is only valid at peak coherence and without the phase correction, the tolerance on radial alignment between ECE and reflectometer position is only a small fraction of the radial correlation length ($< \pm 0.4 L_r$ or $< \pm$ 2-4 mm), despite the fact that the reflectometer is sensitive to fluctuations over a broader radial range than the ECE. This degree of alignment can only be achieved with a channel comb in either ECE or reflectometer, or by painstakingly repeating the measurement with minute adjustments to achieve the same result.

4 Conclusions

A new Correlation ECE (CECE) and density temperature phase angle, α_{nT}, diagnostic has been designed and built for ASDEX upgrade. The system uses 24 non-overlapping frequency channels arranged in a comb pattern, which when radiation transport is considered, give near continuous radial coverage of a small radial region. This diagnostic gives detailed measurements of the radial correlation length of the temperature fluctuations $L_r(T_{e\perp})$ and confirms for the first time the proportionality of $L_r(T_{e\perp})$ to the local thermal ion gyroradius ρ_s. The addition of 2 W-band and 1 V-band X-mode reflectometers along the same line of sight allows the measurement of the phase angle between density and temperature fluctuations α_{nT}. The channel comb significantly improves the reliability of the diagnostic, and it has been shown that the condition of radial alignment can be more stringent than previously thought due to a linear trend in the cross-phase as a function of the separation between reflectometer cut-off and ECE channel position. The ECE-ECE cross-phase can be used to correct this phase drift and provide a more robust measurement. High fidelity, ion-scale, non-linear gyrokinetic simulations performed agree well with the experimentally inferred electron and ion heat fluxes, while simultaneously matching the measured α_{nT} and $L_r(T_{e\perp})$. Temperature fluctuation amplitudes are slightly above those measured in the plasma.

Acknowledgements

This work is supported by the US DOE under grants DE-SC0006419 and DE-SC0017381, and was performed in the framework of the Helmholtz Virtual Institute on Plasma Dynamical Processes and Turbulence Studies using Advanced Microwave Diagnostics. It has also been carried out within the framework of the EUROfusion Consortium and has received funding from the Euratom research and training programme 2014-2018 under grant agreement No 633053. The views and opinions expressed herein do not necessarily reflect those of the European Commission.

References

[1] J. Connor, H. Wilson, Plasma Physics and Controlled Fusion **36**, 719 (1994)

[2] W. Horton, Reviews of Modern Physics **71**, 735 (1999)

[3] A. White, W. Peebles, T. Rhodes, C. Holland, G. Wang, L. Schmitz, T. Carter, J. Hillesheim, E. Doyle, L. Zeng et al., Physics of Plasmas **17**, 056103 (2010)

[4] M. Häse, M. Hirsch, H.J. Hartfuss, Review of Scientific Instruments **70**, 1014 (1999)

[5] J. Hillesheim, J.. DeBoo, W. Peebles, T. Carter, G. Wang, T. Rhodes, L. Schmitz, G. McKee, Z. Yan, G. Staebler et al., Physics of Plasmas **20**, 056115 (2013)

[6] S.J. Freethy, T. Görler, A.J. Creely, G.D. Conway, S.S. Denk, T. Happel, C. Koenen, P. Hennequin, A.E. White, Physics of Plasmas **25**, 055903 (2018)

[7] F. Jenko, W. Dorland, Plasma Physics and Controlled Fusion **43**, A141 (2001)

[8] L. Porte, S. Coda, T. Goodman, A. Pochelon, V. Udintsev, V. Vuille, EPJ Web of Conferences **32**, 03007 (2012)

[9] M. Fontana, L. Porte, S. Coda, O. Sauter, Nuclear Fusion **58**, 024002 (2018)

[10] T.L. Rhodes, J.N. Leboeuf, R.D. Sydora, R. Groebner, E.J. Doyle, G.R. McKee, W.A. Peebles, C.L. Rettig, L. Zeng, G. Wang, Phys. Plasmas **9**, 2141 (2002)

[11] S. Denk, R. Fischer, O. Maj, E. Poli, J. Stober, U. Stroth, B. Vanovac, W. Suttrop, M. Willensdorfer, EPJ Web of Conferences **147**, 02002 (2017)